

Responsive Photonic Liquid Crystalline Flakes Produced by Ultrasonication

Citation for published version (APA):

Sol, J. A. H. P., Kessels, L., del Pozo Puig, M., & Debije, M. G. (2021). Responsive Photonic Liquid Crystalline Flakes Produced by Ultrasonication. *Advanced Photonics Research*, 2(4), Article 2000115.
<https://doi.org/10.1002/adpr.202000115>

Document license:

CC BY

DOI:

[10.1002/adpr.202000115](https://doi.org/10.1002/adpr.202000115)

Document status and date:

Published: 07/04/2021

Document Version:

Publisher's PDF, also known as Version of Record (includes final page, issue and volume numbers)

Please check the document version of this publication:

- A submitted manuscript is the version of the article upon submission and before peer-review. There can be important differences between the submitted version and the official published version of record. People interested in the research are advised to contact the author for the final version of the publication, or visit the DOI to the publisher's website.
- The final author version and the galley proof are versions of the publication after peer review.
- The final published version features the final layout of the paper including the volume, issue and page numbers.

[Link to publication](#)

General rights

Copyright and moral rights for the publications made accessible in the public portal are retained by the authors and/or other copyright owners and it is a condition of accessing publications that users recognise and abide by the legal requirements associated with these rights.

- Users may download and print one copy of any publication from the public portal for the purpose of private study or research.
- You may not further distribute the material or use it for any profit-making activity or commercial gain
- You may freely distribute the URL identifying the publication in the public portal.

If the publication is distributed under the terms of Article 25fa of the Dutch Copyright Act, indicated by the "Taverne" license above, please follow below link for the End User Agreement:

www.tue.nl/taverne

Take down policy

If you believe that this document breaches copyright please contact us at:

openaccess@tue.nl

providing details and we will investigate your claim.

Responsive Photonic Liquid Crystalline Flakes Produced by Ultrasonication

Jeroen A. H. P. Sol, Lana M. Kessels, Marc del Pozo, and Michael G. Debije*

Responsive materials that alter their color in response to environmental changes can be used as optical sensors. Chiral nematic liquid crystals are photonic materials that selectively reflect specific wavelengths of light and have been made environmentally responsive. Herein, the use of ultrasonication of responsive cholesteric liquid-crystal network films to form structurally colored flakes that demonstrate color changes when moved from an aqueous to dry environment and back again is demonstrated, which suggests a scalable technique to form quantities of responsive particles that could conceivably be embedded in permeable hosts to allow the optical detection of humidity or certain chemical species.

1. Introduction

The perception of color has played a critical role in human development, helping the earliest peoples to judge the ripeness of food, vital for their safety.^[1,2] For this reason, human vision has evolved to be most sensitive in the range of 380–780 nm.^[3] Colors can result from light absorbance or luminescence by pigments, or photonic systems that generate vivid colors via selective reflection of regions of the electromagnetic spectrum as a result of nanoscale arrangement of their constituent materials.^[4] Using structural color rather than pigments or luminophores has some key advantages. Dyes and pigments influence the light spectrum by absorption of photons and dissipate this absorbed energy as heat, re-emission of lower energy photons, or by breaking chemical bonds. The latter process—photobleaching—is primarily responsible for colors fading over time. For structural color, as long as the structure persists, the color remains observable. The structured materials may also be dynamic: when the material is swelled or contracted by exposure to environmental factors, the


result may be dramatic color changes, which could be harnessed for use as sensors.^[5]

Self-assembling liquid crystals (LCs) in the chiral nematic, “cholesteric” (ChLC) phase have been utilized to fashion reflective materials. ChLCs selectively reflect a narrow bandwidth (normally 75–100 nm in the visible spectrum) of incident light with a polarization matching the twist of the cholesteric helical structure (left or right handed); thus, up to 50% of unpolarized incident light of that wavelength.^[6] Through proper selection of molecular constituents, the ChLCs can be made

responsive to CO₂, temperature, UV radiation, humidity, or a number of other triggers so the reflection alters after exposure, sometimes reversibly and sometimes irreversibly.^[7,8] By polymerizing the reactive ChLC monomers into a ChLC network (ChLCN), one makes a step toward materials applicable as photonic plastics. Almost always described in thin-film format, these materials have served as visual security features,^[9] and indicators for temperature,^[10,11] medical conditions (hypo/hypercalcemia^[12]) or presence of chemical analytes, such as volatile low molecular weight amines.^[13] Furthermore, due to their vibrant, angular-dependent color, ChLC materials have been used in the decorative coatings industry as effect pigments,^[14] and recently as responsive cholesteric networks coatings.^[15] An alternative cholesteric coating is based on spherical particles embedded in a binder, although a high concentration of the particles is required—with a very specific LC alignment pattern.^[16] In this work, we present a process that will allow broader application of a wide variety of ChLC-based materials by generating small form factor responsive flakes that can be used as dopants for otherwise static hosts to expand their use toward sensing applications.

LC network flakes have found use in display technology^[17–21] as well as decorative elements.^[22,23] A variety of manufacturing methods have been described, including cryogenic^[22] and mechanical^[24,25] fracturing, and soft lithography.^[17,21,26] Ultrasonication, a technique used in cellular biology and chemistry to release cell contents by rupturing cell membranes^[27] and as method to deaggregate nanoparticles,^[28] has been presented once, but not for responsive photonic LC networks.^[29] Herein, we present ultrasonication as a viable method of reducing the ChLCN film dimensions while preserving the stimulus-responsive color change capabilities of the particles and show thorough characterization of the material along all steps of fabrication and incorporation in a binder material.

J. A. H. P. Sol, L. M. Kessels, M. del Pozo, Dr. M. G. Debije
Laboratory of Stimuli-Responsive Functional Materials and Devices
Department of Chemical Engineering & Chemistry
Eindhoven University of Technology
5600 MB Eindhoven, The Netherlands
E-mail: m.g.debije@tue.nl

 The ORCID identification number(s) for the author(s) of this article can be found under <https://doi.org/10.1002/adpr.202000115>.

© 2020 The Authors. Advanced Photonics Research published by Wiley-VCH GmbH. This is an open access article under the terms of the Creative Commons Attribution License, which permits use, distribution and reproduction in any medium, provided the original work is properly cited.

DOI: 10.1002/adpr.202000115

2. Results and Discussion

2.1. Photonic Film Fabrication

The photonic ChLCN films were made by combining two reactive mesogens, **1** and **2**, with chiral dopant **3** to induce a helical twist in the nematic structure of the LC (see **Figure 1** for the chemicals used in this work). Hydrogen-bonded dimers of **4** and **5** were added to allow for reversible reduction of the cross-linking density in the film as well as tuning its polarity with the goal of sensitizing the reflected color to H₂O content. Nonreactive mesogen **6** is added as a sacrificial species: before and during polymerization, it helps maintain liquid crystalline order, whereas after fashioning of the film, it is removed to leave behind a permeable interior in the ChLCN film. Photoinitiator **7** initiates the free radical polymerization that links up the acrylate groups, immobilizing the photonic ChLC alignment.

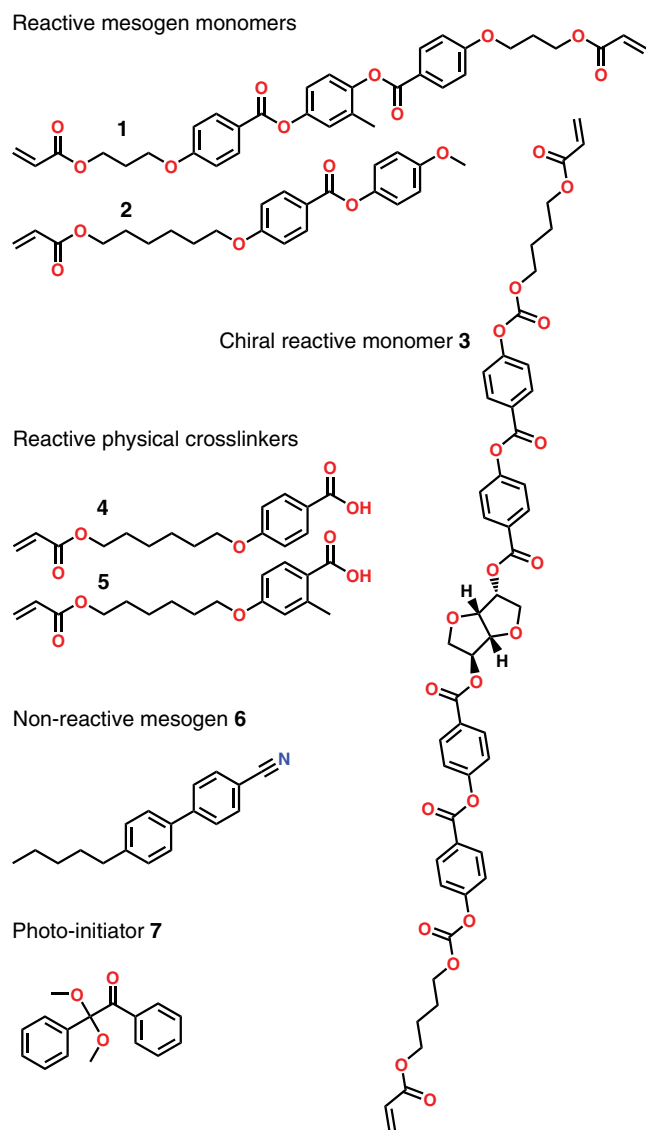


Figure 1. The chemical structures of the molecules used in this work.

Depending on the size of cholesteric film desired, up to 100 μL of monomer mixture was placed on a glass slide heated to 80 $^{\circ}\text{C}$, above the cholesteric-isotropic transition temperature of the LC mix (see **Figure S1**, Supporting Information, for differential scanning calorimetry [DSC] trace). Shearing the LC mixture between poly(vinyl alcohol) (PVA)-coated glass substrates gave rise to a vibrant photonic reflectors that was retained after polymerization with intense ultraviolet light (photonic $\lambda_{\text{max}} \approx 605 \text{ nm}$, **Figure 2a**). Acrylate conversion went to completion, confirmed by the disappearance of the Fourier-transform infrared (FT-IR) signature peak for the acrylate ($\tilde{\nu} \approx 985, 1410 \text{ cm}^{-1}$) (**Figure 2b**).^[30] Placing the polymerized cell filled with solid film in 50 $^{\circ}\text{C}$ water, the PVA sacrificial layer quickly dissolved, releasing the ChLCN. After soaking in tetrahydrofuran (THF), porogenic, non-reactive compound **6** was removed (confirmed using FT-IR, **Figure 2b**, $\tilde{\nu} \approx 2225 \text{ cm}^{-1}$), resulting in partial collapse of the network and a subsequent blue shift of the reflection (to $\lambda_{\text{max}} \approx 480 \text{ nm}$, **Figure 2c**). A treatment with an alkaline K^+OH^- solution (0.1–1 M in H₂O) resulted in a strongly hygroscopic network that easily absorbs moisture from the surrounding air (for instance by breathing over the film surface) or when placed in water. FT-IR confirms scission of the hydrogen-bonded carboxylic acid dimers ($\tilde{\nu} \approx 1680 \text{ cm}^{-1}$) as well as the formation of a polymer salt featuring negatively charged carboxylates ($-\text{CO}_2^-$, at $\tilde{\nu} \approx 1380, 1550 \text{ cm}^{-1}$).^[12] The maximum of the selective reflection band shifted to $\lambda_{\text{max}} \approx 500 \text{ nm}$ after treatment. Subsequent soaking in water of the lye-exposed film reveals a red color ($\lambda_{\text{max}} = 600 \text{ nm}$). From past work, it is known that these color shifts are directly related to the physical swelling and deswelling of the polymer network.^[9,31] As confirmed using circular polarized UV–vis measurements, the cholesteric LC (ChLC) retains most of its characteristic circular dichroism, and SEM images indicate molecular order and internal structural integrity is maintained in all states from the pristine film to the swollen polymer salt (**Figure S2** and **S3**, Supporting Information). From the UV–vis data in **Figure S3**, Supporting Information, narrowing of the reflection bands is seen, an effect resulting from the loss of birefringence during formation of the polymer salt.^[32] In addition, FT-IR results show no significant weakening of the ester bond peaks (see $\tilde{\nu} \approx 1730 \text{ cm}^{-1}$ for $\text{C}=\text{O}$, $\tilde{\nu} \approx 1200\text{--}1300 \text{ cm}^{-1}$ for $\text{C}-\text{O}-\text{C}$ bonds). As described previously for this ChLC composition, the polymer salt can be reverted back into a hydrogen-bonded material through an acid treatment, using for instance aqueous HNO_3 ; we demonstrate partial reversion after a 90 min exposure (see **Figure 2c**).^[9]

2.2. Fracturing of ChLCN Films into Photonic Flakes and Photonic Response

After removal from the LC polymerization cell, the films were transferred to a vial filled with demineralized water ($\approx 5 \text{ mL}$). The sonication probe tip was placed in the liquid and ultrasonication initiated. Within the first few seconds, the large centimeter-sized film breaks up into a myriad of small pieces (see **Video S1**, Supporting Information).

The size of the flakes is quantified using digital image analysis. During and after ultrasonication, samples were taken from the aqueous flake dispersion, dried on a glass slide and imaged

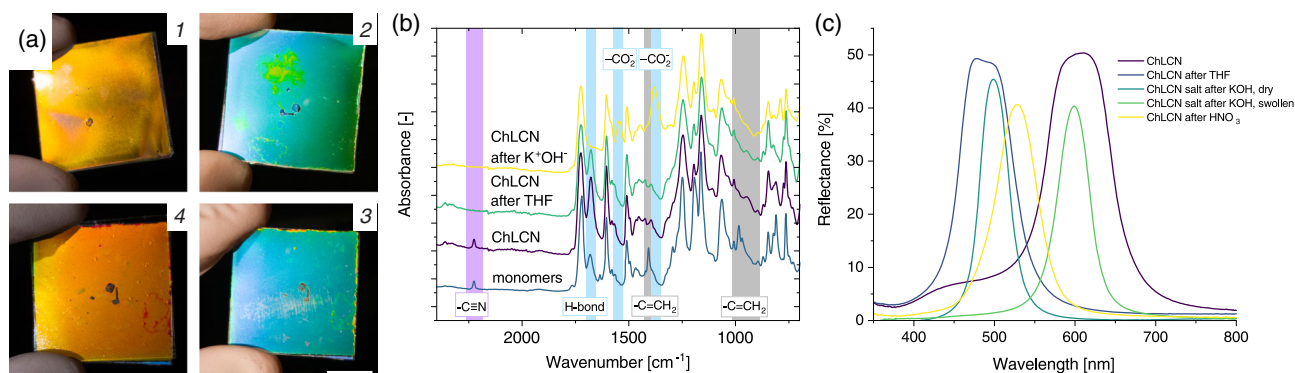


Figure 2. a) Clockwise from top left: ChLCN coating after polymerization (1), after porogen **6** extraction (2), after 0.1 M K⁺OH⁻ treatment and drying to air (3), and after swelling in water (4). The scale bar corresponds to 10 mm. b) FT-IR spectroscopy before (blue line), and after photo-induced crosslinking (violet line, N.B. 985, 1410 cm⁻¹), after extraction of porogenic mesogen **6** (green line, N.B. 2225 cm⁻¹), and after treatment in 0.1 M K⁺OH⁻ solution (yellow line, N.B. 1380, 1550, 1680 cm⁻¹). c) UV-vis spectroscopy after each processing step of the ChLCN material: the initial film (violet line), after the THF treatment (blue line), after 1.0 M KOH treatment which opens the pores, dried (turquoise), after swelling (green) and after 0.5 M aqueous HNO₃ treatment to close the hydrogen bonds in the ChLCN (yellow).

using polarized optical microscopy (POM). Between crossed polarizers, the brightly colored Grandjean texture provides good contrast with the dark background, which greatly eases the image analysis procedure. Micrographs for each sample were analyzed to give a mean Feret's diameter value for the set, as well as the deviation within the sample. The Feret's diameter that the analysis software reports in this case is the diameter of the smallest circle that entirely circumscribes the imaged particle, and this is a measure of the length of a particle along its longest axis. For proposed applications as a dopant in fused filament fabrication (FFF), we feel that this is a useful metric as one wishes to prevent particles becoming stuck in the print head; for a conventional FFF 3D printer as utilized here the nozzle diameter is 400 μm.

Samples collected throughout the ultrasonication procedure show that the median Feret diameter decreases with sonication time (Figure 3) up to a point. After ≈55 min of ultrasonication of 0.1 M K⁺OH⁻-treated polymer, a steady state of about 150 ± 75 μm is found. The storage modulus *E'* of hydrogen-bonded LC films drops significantly after base treatment,^[33] we assume fracturing efficiency to be dependent on the “softness” of the material. As expected, fracturing proceeds more slowly and yields larger flakes for the untreated ChLCN films compared with the K⁺OH⁻-treated films. Using a microporous glass filter (10–16 μm pore size), the flakes were removed from the aqueous dispersion and washed with demineralized water and dried to obtain a polymer powder. Scanning electron microscopy (SEM) photographs show the photonic periodicity in the polymer film remains intact throughout the ultrasonication procedure (Figure S3, Supporting Information).

A study of film thickness on ultrasonication efficiency revealed no significant correlation: for films made in 6, 10, or 20 μm gap cells, median Feret's diameters of 189, 198, and 176 μm were found after 40 min of ultrasonication, respectively. Similarly, larger ChLCN films fabricated in 69 × 69 mm² cells were sonicated using an identical procedure and resulted in similar median Feret's diameters of 160 μm. Processing multiple individual films in a single batch demonstrated at least four large films (±200 mg) can be fractured simultaneously without

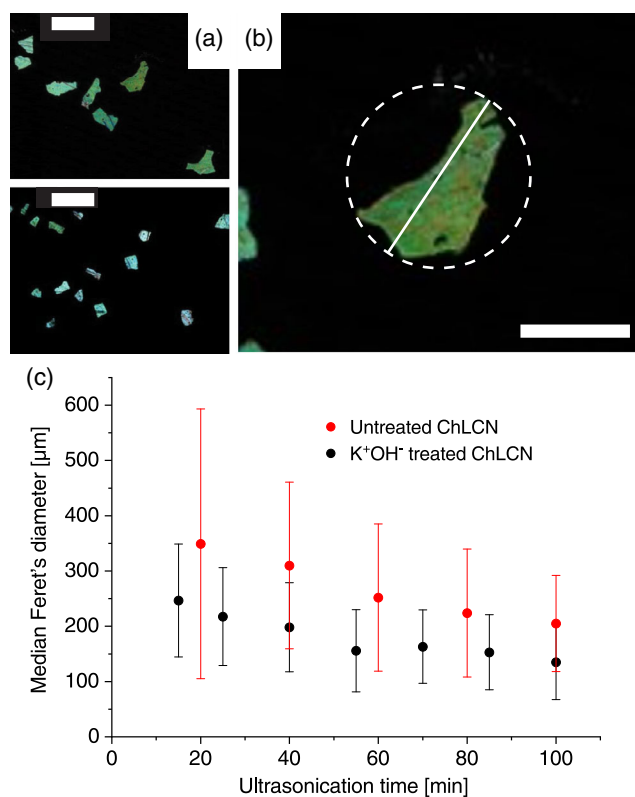


Figure 3. a) Optical microscopy images taken between crossed polarizers of the dry ChLCN flakes observed after 15 min (top) and 100 min (bottom) ultrasonication. The scale bar corresponds to 500 μm. b) Detail of the image in (a): example of how Feret's diameters are calculated. The scale bar corresponds to 250 μm. c) The ChLC particle Feret's diameter versus ultrasonication time for untreated (red) and K⁺OH⁻-treated material (black).

significantly affecting the final flake sizes. In terms of upscaling, this means that flake production rates can be increased more than an order of magnitude (from 10 mg per 30 × 30 mm² film,

to 200 mg for 4 films of $69 \times 69 \text{ mm}^2$) without changing the procedure or its parameters. Interestingly, in some cases, we observed that flakes formed during ultrasonication were green instead of red, the expected color for the material in its fully hydrated state. Using FT-IR spectroscopy, it was confirmed that this is a result of hydrogen bond reformation ($\tilde{\nu} \approx 1680 \text{ cm}^{-1}$), a reaction that could be easily reversed by treating these flakes with $0.1 \text{ M K}^+\text{OH}^-$ solution.

The flakes, after filtration from the sonication medium and a washing step in demineralized water, show the same responsive behavior as seen for the intact films (Figure 4a). In the dry polymer salt state, a green reflection is observed which red shifts within seconds after wetting the flakes. Drying is done under ambient conditions but can be sped up by heating the material, in this case with a heating plate at 100°C , which removed water from the cholesteric particles within seconds, reverting the color to green. In situ UV-vis spectrophotometry was used to record light reflection spectra of the flakes at different humidity and temperature conditions. Figure 4b and Figure S4, Supporting Information, clearly demonstrate that at constant temperature, the wavelength of maximal reflection is strongly dependent on the surrounding humidity, shifting from $\approx 570 \text{ nm}$ at 40 RH% to 630 nm at 80 RH%. As shown in prior research, below 40 RH%, no significant shift in the reflection band occurs.^[31,34] The same effect can be achieved by maintaining a constant humidity level and lowering the temperature (see Figure 4c and Video S2, Supporting Information). This shift relies on the condensation of water into the flakes. An atmosphere with

75 RH% at an air temperature of 23°C has a dew point temperature of 18°C ^[35,36]; this means that when the flakes are cooled from 50°C , the evaporation rate of water from the flake progressively decreases, gradually filling the polymer with moisture. Upon crossing the dew point (i.e., $T \leq 18^\circ\text{C}$), the water condensation rate surpasses the evaporation rate leading to water droplets forming onto the flakes and causing maximum swelling and red shift, as is shown clearly in Figure 4c. As shown in Figure S4, Supporting Information, the wavelength shift when changing the relative humidity level follows a linear trend, while changing the temperature at constant relative humidity shows an exponential curve.^[31]

Although not demonstrated here, the chemistry used for these responsive flakes could allow for tunable crosslinking using calcium(II) ions, for example, in the future.^[9] Divalent Ca^{2+} species bonds two carboxylic acid groups: combined with the high degree of order in this liquid crystalline network, the concentration of Ca^{2+} significantly influences the degree of water uptake by the material, and thus should also influence the maximum wavelength shift between dry and wet states.

2.3. Toward Applications for ChLCN Flakes

In all previously reported cases where ChLC flakes are used as optically active components for flexible reflective displays,^[17,19,21,26,37] windows,^[29] circular polarization-dependent security labels,^[11] or as effect pigments for decorative coatings,^[14] the cholesteric material is based on a

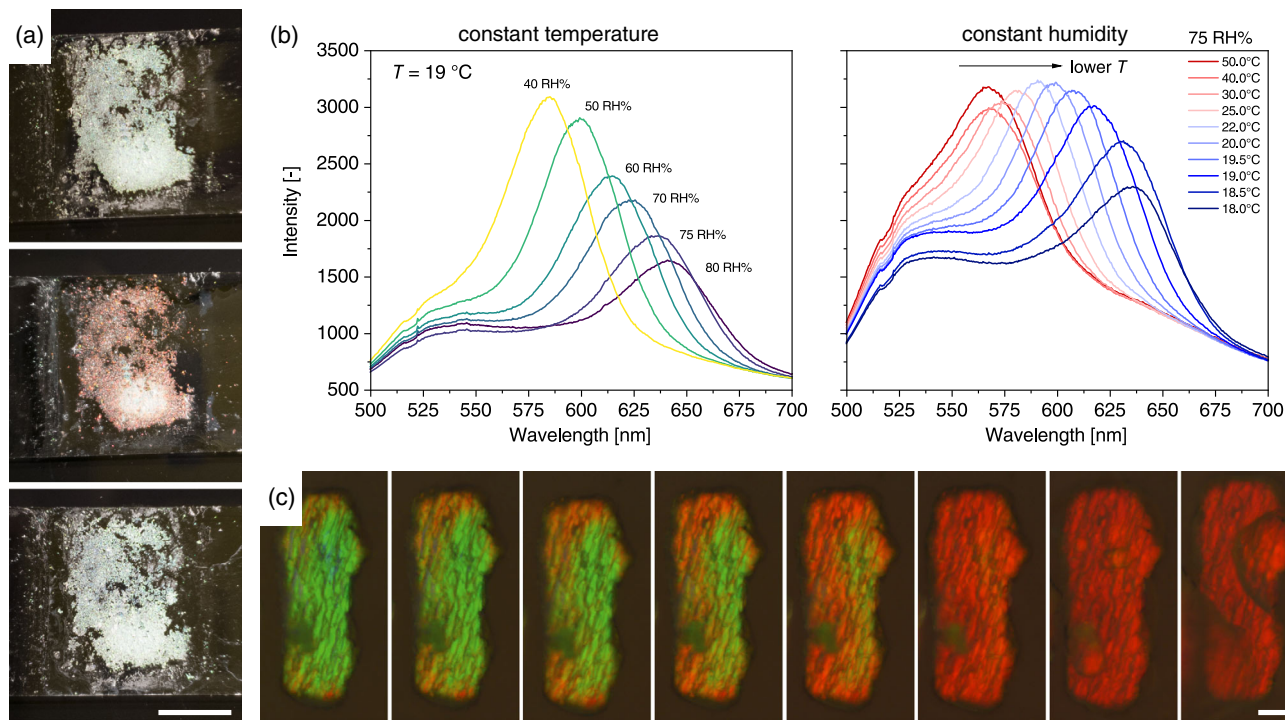


Figure 4. a) ChLC flake powder in the dry state (top), after soaking in demineralized water (middle), and after drying on a 110°C hot plate. The scale bar corresponds to 10 mm. b) Left, UV-vis reflectance spectra of a single ChLC flake at a constant temperature ($T = 19^\circ\text{C}$) for increasing levels of relative humidity (from 40 to 80 RH%). Right, UV-vis reflectance spectra for a single flake at constant relative humidity (75 RH%) at different temperatures (from 18 to 50°C). c) Optical polarized microscopy photographs of the flake analyzed at constant relative humidity (75 RH%) for different temperatures (see (b)) starting at 50°C (leftmost) and ending at 18°C (rightmost). The scale bar corresponds to 20 μm .

densely crosslinked polymer network with a static photonic structure.

The material described in this article is similar to the flakes described in the aforementioned reports, but with the added feature of optical responsivity to environmental stimuli in the presence of water after breaking the supramolecular physical crosslinks formed through hydrogen bonding. During the color change from green to red, the material fills with H₂O, causing swelling along the direction of the photonic cholesteric helix. This makes incorporation in conventional matrices difficult, as there is need for both permeability to moisture, as well as room for the photonic particles to swell.

Nevertheless, to demonstrate the processability of these responsive flakes, we compounded them with poly(lactic acid) (PLA) into a FFF 3D printing filament, at a 1% w/w ratio ChLC flake to polymer matrix. Flakes were produced in 69 × 69 mm² cells to generate larger amounts of photonic material. These were activated, sonicated, and dried and added to about 50 g PLA granulate. Mixing was carried out by hand, after which the granular blend was poured into a compounder set to output a 2.85 mm diameter filament (Figure 5a,b). As shown in the photograph, the flakes are well dispersed in the filament. After using this filament to print 3D objects, the flakes can be observed through POM as well as visually (Figure 5b,c). For additional information regarding the compounding of the flakes and the 3D printing procedure using PLA-flake composite filament, we refer to Figures S5–S8, Supporting Information, and the accompanying text.

The processability limits of these flakes do pose some issues, as hinted at by thermogravimetric analysis (TGA) (Figure S9, Supporting Information). The flake material is heated and maintained at 200 °C and kept isothermally for 20 min to simulate filament extrusion and printing procedures. At this point, 11% of the original mass is lost in the form of evaporated H₂O. Otherwise, the material is stable, showing no other ill-effects from the treatment, indicating it is suitable for incorporation in low melting point polymers, such as PLA, as demonstrated. The composite was processed at 190 °C and printed at 200 °C. However, the barrier properties of PLA, with limited moisture uptake, limit functionality of the responsive photonic dopant.^[38]

Trials with a high melting point but more hydrophilic polymer, polyamide-6 (PA6),^[39] showed that these stability limits were exceeded, as no flakes could be visually identified in the

resulting filament. This is likely due to the prolonged exposure to higher temperatures in the filament extruder (±260–270 °C). At these temperatures, terminal degradation of the cholesteric polymer flakes sets in (see Figure S9, Supporting Information).

To show that responsivity may be maintained after incorporation of the photonic dopant in an appropriate polymer host, the flakes were dispersed in an aqueous solution of PVA at 5% w/w ChLCN flakes to PVA. A coating was applied onto a glass substrate via solvent casting, which, after drying, clearly shows the green reflection from the dried ChLCN flakes (Figure 6). As the PVA is not immediately susceptible to water penetration at room temperature, response of the PVA-flake composite coating was tested at 80 °C. At this temperature, dropping water on the coating leads to fast absorption of the liquid into the ChLC flakes which swell and change color (steps 1 to 2 and 3). As the material is at a high temperature, water eventually evaporates after a few minutes, reverting the coating to its initial state (steps 2 to 3, and then 4). The rewritability of this coating has been

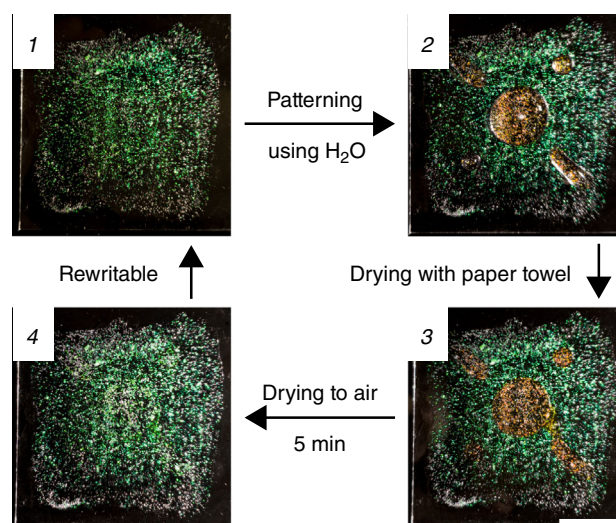


Figure 6. Rewritable coating demonstrated at 80 °C. Clockwise from top left: a dry PVA-coating is patterned using demineralized water (1–2), excess water is removed using a paper towel, showing that water has penetrated into the coating and the ChLCN flakes (2–3). After a couple of minutes, water evaporates from the sample (3–4), which returns it to its initial state (4–1). The scale bar corresponds to 20 mm.

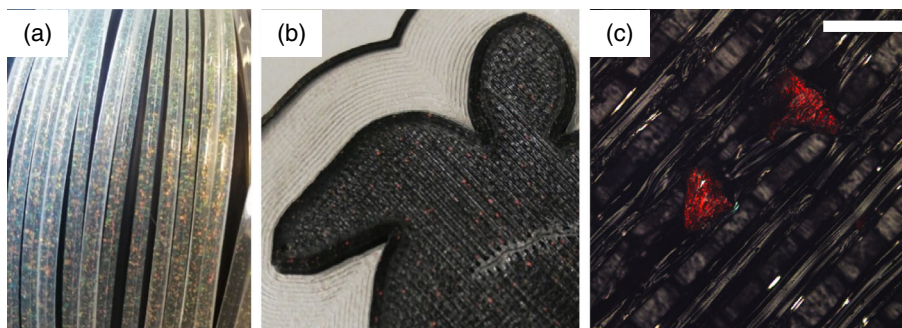


Figure 5. a) A 2.85 mm PLA filament with incorporated photonic cholesteric flakes. b) 3D object printed using black PLA as support with a single layer of photonic flake-doped, transparent PLA. c) POM photograph of the projected object in reflection mode showing the incorporation of the flakes in the isotropic polymer host. The scale bar corresponds to 500 μm.

further explored in Figure S10, Supporting Information. Such a film could be used as visual temperature indicator.

3. Conclusions

We have reported a method for the fabrication of stimulus-responsive photonic flakes from liquid crystalline polymer networks. Using ultrasonication, a simple and accessible technique, large polymer films are fractured into small pieces. It was shown that performing a base treatment on the flakes before ultrasonication gave smaller flakes on average; additional time-controlled tests show that the size of the flakes plateaus after about an hour at around 150 μm , a size at which the flakes can be incorporated in other media while keeping good optical visibility, as demonstrated for PLA-based 3D printing filament. However, the flakes require sufficient space to swell with water, which favors certain polymer host matrices over others. To demonstrate the function of these flakes, we have demonstrated a rewritable coating based on a PVA binder doped with these photonic particles that shows a reversible optical response to hot water. The optical response in the cholesteric flakes is a large shift in the central wavelength of the selective reflection band, from green ($\lambda_{\text{max}} = 570 \text{ nm}$) to red ($\lambda_{\text{max}} = 630 \text{ nm}$).

4. Experimental Section

Materials: Reactive LC mesogens **1** (2-methyl-1,4-phenylene bis(4-(3-(acryloyloxy)propoxy)benzoate)) and **2** (4-methoxyphenyl 4-((6-(acryloyloxy)hexyl)oxy)benzoate) were obtained from Merck KGaA. Reactive chiral dopant **3** ((3*R*,3*aR*,6*S*,6*aR*)-hexahydrofuro[3,2-*b*]furan-3,6-diyl bis(4-((4-((4-(acryloyloxy)butoxy)carbonyl)oxy)benzoyl)oxy)benzoate)) was purchased from BASF SE. Hydrogen-bonded reactive LC **4** (4-((6-(acryloyloxy)hexyl)oxy)benzoic acid) was purchased from Synthon Chemicals GmbH & Co. KG and Ambeed Inc. Hydrogen-bonded reactive LC **5** (4-((6-(acryloyloxy)hexyl)oxy)-2-methylbenzoic acid) was purchased from Synthon Chemicals GmbH & Co. KG. Nonreactive porogenic LC **6** (4-cyano-4'-pentylbiphenyl) was purchased from TCI Chemicals Europe N.V. Photoinitiator **7** (2,2-dimethoxy-2-phenylacetophenone) was purchased from BASF SE. See Figure 1 for structures of the components. KOH pellets and PVA granulate (MW 31 000–50 000, 87–89% hydrolyzed) were purchased from Sigma-Aldrich Inc. THF was purchased from Biosolve B.V. PLA was purchased from NatureWorks LLC (Ingeo 4043D). Polyamide-6 (PA6) was cordially gifted by Royal DSM N.V. (Akulon F136).

LC Alignment Cells: Glass substrates were cleaned with a two-step procedure: first 20 min of ultrasonication in 1:1 v/v 2-propanol/ethanol, followed by 20 min in a UV/O₃-oven (UV Products PR-100). Clean glass substrates (borosilicate 30 × 30 mm² or soda-lime 69 × 69 mm²) were coated with either a PVA solution (4 wt% in H₂O) through spin coating at 1500 rpm for 30 s (Karl Suss RC6), or for analysis, 3-(trimethoxysilyl)propyl methacrylate (1 vol% in 1:1 v/v ratio 2-propanol/water) at the same spin settings. UV-curable glue to control the cell gap was made by mixing glue (UV Sealant 91, Norland Products Inc.) with resin spacer beads of varying diameter (6, 10, 20 μm ; Micropearl SP series, Sekisui Chemical Co., Ltd.).

LC Mixture: The liquid crystalline mixture has been described previously:^[9] it combines the base components in THF in the following amounts: 17.9 wt% diacrylate mesogen **1**, 22.9 wt% monoacrylate mesogen **2**, 4.6 wt% chiral diacrylate **3**, 18.0 wt% of both hydrogen-bonded physical crosslinkers **4** and **5**, 18.0 wt% porogenic nonreactive mesogen **6**, 0.6 wt% of photoinitiator **7**. THF was removed from the mixture by evaporation at 80 °C under an air flow, followed by a 50 °C vacuum.

LC Network: Production of cholesteric polymer films was initiated by heating the monomer mixture and glass substrate to 80 °C. Using a

micropipette, 20 μL (30 × 30 mm²) or 100 μL (69 × 69 mm²) of the isotropic monomer mix was transferred to the activated glass substrate. Depending on the experiment, different spacer glues were used (“no spacer glue”, or “glue with no spacers”, or “glue with 6, 10, or 20 μm spacers”), small dots of which were placed near the corners of the bottom glass slide. At this point, the sample was removed from the hot plate, and a second glass substrate was placed on top of the isotropic mix and sheared uniaxially to mechanically align the cholesteric mixture. After short equilibration at room temperature, high intensity UV light (35 mW cm⁻² at sample, Lumen Dynamics EXFO Omnicure S2000) irradiated the sample for 5 min. Films on PVA-treated glass were removed by submersion in demineralized H₂O for 30 min.

Cholesteric Film Activation: The cholesteric polymer films were washed with THF to remove nonreactive mesogen **6**, after which the thin film was dried in air overnight. A subsequent soaking in 100 mM K⁺OH⁻ in H₂O (pH \pm 13) for 60 min created the responsive photonic material.

Cholesteric Film Breakup: K⁺OH⁻-activated polymer films made in 69 × 69 mm² cells were put in a vial filled with demineralized H₂O. An ultrasonic probe (Sonics VC-750 driver with Sonics 630-0418 tapered microtip) was placed in the vial and activated for a variable amount of time in a pulse-wise fashion (2.0 s sonication, 0.5 s rest). Sonicating tip amplitude was set to 35%, to prevent it from overheating. Using a fritted glass filter funnel (ROBU VitraPOR Por. 4), the flakes were separated from the aqueous medium they were fractured in.

Cholesteric Flake Size Quantification: After ultrasonication, samples of the aqueous flake dispersion were taken from the vial using a plastic pipette and placed on a clean microscope slide. Water was removed by heating the slide to 100 °C on a hot plate. POM was used to obtain representative sample images, which were processed using ImageJ/Fiji^[40,41] and an in-house written macro (see Supporting Information). The main quantifier for the flake size is “Feret’s diameter.”^[42]

Materials Characterization: DSC was carried out using a TA Instruments DSC Q2000. TGA was carried out using a TA Instruments TGA Q500 in aerobic conditions. ATR FT-IR spectroscopy was done using a Varian Excalibur 3100 (Ge ATR crystal). POM was done using a Leica DM6000 M. In situ POM and UV–vis spectrophotometry at different temperatures and humidity conditions were carried out using a Leica DM2700 M microscope, fitted with a Leica MC170 HD camera, a Linkam TMS 600 temperature-controlled sample stage and a Sensirion SHT3x temperature/humidity sensor. The sample environment was enclosed using a custom-built transparent humidity chamber. Surface profiles of the films were measured with a Veeco DektakXT. Optical characteristics were measured with a PerkinElmer Lambda 750, a Shimadzu UV-3012 PC fitted with linear polarizer- $\lambda/4$ waveplate stack for circular dichroism measurements, and an OceanOptics HR2000+ optical microscope-attached photospectrometer for in situ measurements. During these in situ measurements, the microscope is operated in bright-field reflection mode with the sample between crossed polarizers as explained in the study by del Pozo et al.^[31] SEM photographs were recorded by sputter-coating material with Au and subsequently imaging it using a FEI Quanta 3D scanning electron microscope.

3D Print Filament Fabrication: Filaments were compounded using a 3Devo NEXT 1.0 extruder. Cholesteric flakes were mixed manually with the polymer before loading into the extrusion column (1% w/w flakes in polymer). The following extruder settings were used for PLA: $T_4 = 170 \text{ }^\circ\text{C}$, $T_3 = 185 \text{ }^\circ\text{C}$, $T_2 = 190 \text{ }^\circ\text{C}$, $T_1 = 180 \text{ }^\circ\text{C}$ (4–3–2–1 from material inlet to extrusion die), screw speed 5.0 rpm, fan speed 70%, filament diameter $\varnothing = 2.85 \text{ mm}$; and for PA6: $T_4 = 270 \text{ }^\circ\text{C}$, $T_3 = 272 \text{ }^\circ\text{C}$, $T_2 = 261 \text{ }^\circ\text{C}$, $T_1 = 258 \text{ }^\circ\text{C}$, screw speed 3.4 rpm, fan speed 100%, and filament diameter $\varnothing = 2.85 \text{ mm}$.

3D Printing of Responsive Filament: 3D models are prepared in Blender (www.blender.org) and sliced using Ultimaker Cura to get the gcode file. The material is printed using an unmodified Ultimaker 3 through a FFF procedure, with the PLA-flake composite as the feed material. The print bed temperature is set to $T_{\text{bed}} = 60 \text{ }^\circ\text{C}$, nozzle temperature to $T_{\text{nozzle}} = 200 \text{ }^\circ\text{C}$. All other settings are derived from the standard PLA print settings present in Ultimaker Cura. Black filament used for multimaterial structures was Ultimaker PLA Black, purchased from Lay3rs 3DPrinting Eindhoven B.V.

Supporting Information

Supporting Information is available from the Wiley Online Library or from the author.

Acknowledgements

This research was funded by the Netherlands Organization for Scientific Research (NWO) in the framework of the Innovation Fund Chemistry and from the Dutch Ministry of Economic Affairs and Climate Policy in the framework of the PPP allowance. The authors thank Tom Heijmans (Ultimaker B.V.) for the kind donation of an Ultimaker 3 FFF printer as well as lending out the 3Devo NEXT 1.0 FFF filament extruder and for suggestions on material choices and the compounding procedure; also Dr. ir. Tom A. P. Engels (TU/e, Royal DSM N.V.) for valuable discussions and insights as well as donating the polymer granulate used in this work. In addition, the authors acknowledge Dr. ir. Ellen P. A. van Heeswijk (TU/e) for carrying out the TGA measurement, and ir. Simon J. A. Houben (TU/e) for recording scanning electron microscope photographs of the cholesteric flakes.

Conflict of Interest

The authors declare no conflict of interest.

Data Availability Statement

Research data are not shared.

Keywords

additive manufacturing, cholesteric flakes, dopants, effect pigments, liquid crystals, polymer photonics, responsive

Received: October 28, 2020

Revised: December 17, 2020

Published online:

- [1] J. Nathans, *Neuron* **1999**, 24, 299.
- [2] E. J. Gerl, M. R. Morris, *Evol. Educ. Outreach* **2008**, 1, 476.
- [3] D. H. Sliney, *Eye* **2016**, 30, 222.
- [4] P. Vukusic, J. R. Sambles, *Nature* **2003**, 424, 852.
- [5] I. B. Burgess, M. Lončar, J. Aizenberg, *J. Mater. Chem. C* **2013**, 1, 6075.
- [6] G. H. Brown, W. G. Shaw, *Chem. Rev.* **1957**, 57, 1049.
- [7] E. P. A. van Heeswijk, A. J. J. Kragt, N. Grossiord, A. P. H. J. Schenning, *Chem. Commun.* **2019**, 55, 2880.
- [8] D. J. Mulder, A. P. H. J. Schenning, C. W. M. Bastiaansen, *J. Mater. Chem. C* **2014**, 2, 6695.
- [9] M. Moirangthem, A. P. H. J. Schenning, *ACS Appl. Mater. Interfaces* **2018**, 10, 4168.
- [10] F. Chen, J. Guo, Z. Qu, J. Wei, *J. Mater. Chem.* **2011**, 21, 8574.
- [11] Y. Jiang, R. Wilson, A. Hochbaum, J. Carter, in *Optical Security and Counterfeit Deterrence Techniques IV. Proc. SPIE*, Vol. 4677 (Ed: R. L. van Renesse), SPIE, Bellingham, WA **2002**, pp. 247–254.
- [12] M. Moirangthem, R. Arts, M. Merx, A. P. H. J. Schenning, *Adv. Funct. Mater.* **2016**, 26, 1154.
- [13] J. E. Stumpel, C. Wouters, N. Herzer, J. Ziegler, D. J. Broer, C. W. M. Bastiaansen, A. P. H. J. Schenning, *Adv. Opt. Mater.* **2014**, 2, 459.
- [14] F. J. Maile, G. Pfaff, P. Reynders, *Prog. Org. Coat.* **2005**, 54, 150.
- [15] E. P. A. van Heeswijk, L. Yang, N. Grossiord, A. P. H. J. Schenning, *Adv. Funct. Mater.* **2020**, 30, 1906833.
- [16] A. Belmonte, M. Pilz da Cunha, K. Nickmans, A. P. H. J. Schenning, *Adv. Opt. Mater.* **2020**, 8, 2000054.
- [17] A. Trajkovska-Petkoska, R. Varshneya, T. Z. Kosc, K. L. Marshall, S. D. Jacobs, *Adv. Funct. Mater.* **2005**, 15, 217.
- [18] A. Trajkovska-Petkoska, T. Z. Kosc, K. L. Marshall, K. Hasman, S. D. Jacobs, *J. Appl. Phys.* **2008**, 103, 094907.
- [19] K. L. Marshall, K. Hasman, M. Leitch, G. Cox, T. Z. Kosc, A. Trajkovska-Petkoska, S. D. Jacobs, *SID Symp. Dig. Tech. Pap.* **2007**, 38, 1741.
- [20] T. Z. Kosc, K. L. Marshall, S. D. Jacobs, *SID Symp. Dig. Tech. Pap.* **2003**, 34, 581.
- [21] W. Liu, Y. Zhou, S. Liu, W. Shao, D. J. Broer, G. Zhou, D. Yuan, D. Liu, *ACS Appl. Mater. Interfaces* **2019**, 11, 40916.
- [22] E. M. Korenic, S. D. Jacobs, S. M. Fare, L. Li, *Mol. Cryst. Liq. Cryst. Sci. Technol. Sect. A* **1998**, 317, 197.
- [23] E. M. Korenic, S. D. Jacobs, S. M. Faris, L. Li, *Color Res. Appl.* **1998**, 23, 210.
- [24] S. M. Faris, *US5364557*, **1994**.
- [25] D. Coates, M. Goulding, A. May, *US6207770*, **2001**.
- [26] G. Zhou, S. Liu, W. Liu, D. Yuan, G. Zhou, *Micromachines* **2019**, 10, 441.
- [27] R. B. Brown, J. Audet, *J. R. Soc. Interface* **2008**, 5, S131.
- [28] S. Pradhan, J. Hedberg, E. Blomberg, S. Wold, I. Odnevall Wallinder, *J. Nanoparticle Res.* **2016**, 18, 285.
- [29] G. Zhou, D. Yuan, Y. Liu, X. Lin, G. Zhou, N. Li, *Acta Photonica Sin.* **2017**, 46, 331002.
- [30] G. Socrates, *Infrared and Raman Characteristic Group Frequencies: Tables and Charts*, John Wiley & Sons, Chichester **2004**.
- [31] M. del Pozo, C. Delaney, C. W. M. Bastiaansen, D. Diamond, A. P. H. J. Schenning, L. Florea, *ACS Nano* **2020**, 14, 9832.
- [32] B. M. Oosterlaken, Y. Xu, M. M. J. Rijt, M. Pilz da Cunha, G. H. Timmermans, M. G. Debije, H. Friedrich, A. P. H. J. Schenning, N. A. J. M. Sommerdijk, *Adv. Funct. Mater.* **2020**, 30, 1907456.
- [33] O. M. Wani, R. Verpaalen, H. Zeng, A. Priimagi, A. P. H. J. Schenning, *Adv. Mater.* **2019**, 31, 1805985.
- [34] E. P. A. van Heeswijk, J. J. H. Kloos, N. Grossiord, A. P. H. J. Schenning, *J. Mater. Chem. A* **2019**, 7, 6113.
- [35] M. G. Lawrence, *Bull. Am. Meteorol. Soc.* **2005**, 86, 225.
- [36] O. A. Alduchov, R. E. Eskridge, *J. Appl. Meteorol.* **1996**, 35, 601.
- [37] A. Trajkovska-Petkoska, S. D. Jacobs, *Mol. Cryst. Liq. Cryst.* **2008**, 495, 334.
- [38] J. V. Ecker, A. Haider, I. Burzic, A. Huber, G. Eder, S. Hild, *Rapid Prototyp. J.* **2019**, 25, 672.
- [39] R. C. P. Verpaalen, M. G. Debije, C. W. M. Bastiaansen, H. Halilović, T. A. P. Engels, A. P. H. J. Schenning, *J. Mater. Chem. A* **2018**, 6, 17724.
- [40] C. A. Schneider, W. S. Rasband, K. W. Eliceiri, *Nat. Methods* **2012**, 9, 671.
- [41] J. Schindelin, I. Arganda-Carreras, E. Frise, V. Kaynig, M. Longair, T. Pietzsch, S. Preibisch, C. Rueden, S. Saalfeld, B. Schmid, J.-Y. Tinevez, D. J. White, V. Hartenstein, K. Eliceiri, P. Tomancak, A. Cardona, *Nat. Methods* **2012**, 9, 676.
- [42] W. H. Walton, *Nature* **1948**, 162, 329.